

High birefringence liquid crystal mixtures for electro-optical devices

EDWARD NOWINOWSKI-KRUSZELNICKI^{1*}, JERZY KĘDZIERSKI¹, ZBIGNIEW RASZEWSKI¹,
LESZEK JAROSZEWICZ¹, ROMAN DĄBROWSKI¹, MAREK KOJDECKI¹, WIKTOR PIECEK¹,
PAWEŁ PERKOWSKI¹, KATARZYNA GARBAT¹, MAREK OLIFIERCZUK¹, MAREK SUTKOWSKI²,
KAROLINA OGRODNIK¹, PRZEMYSŁAW MORAWIAK¹, EMILIA MISZCZYK³

¹Military University of Technology, ul. gen. S. Kaliskiego 2, 00-908 Warsaw, Poland

²Warsaw University of Technology, Plac Politechniki 1, 00-661 Warsaw, Poland

³Radom University of Technology, ul. Malczewskiego 29, 26-600 Radom, Poland

*Corresponding author: enowinowski@wat.edu.pl

High-birefringence nematic liquid crystals recently developed in the Military University of Technology (Poland) are examined for selected physical properties. In particular, for six liquid crystal mixtures there were determined: two components of dielectric permittivity for voltage frequencies in the range from 10 Hz to 10 MHz; rotational viscosity; splay, twist and bend elastic constants; ordinary and extraordinary refractive indices for light wavelengths in the range from 0.3 μ m to 1.6 μ m. The properties are discussed in terms of applicability of the new liquid crystals to electro-optical devices.

Keywords: liquid crystal, birefringence, physical properties.

1. Introduction

Despite the considerable research progress in the last years in the development of nematic liquid crystals, one should also know that there are several tradeoffs, such as limited view angle, brightness, contrast and switching times and that these parameters can be improved further. Liquid crystal materials containing unsubstituted cyclohexylbenzene and bicyclohexyl benzene isothiocyanates, biphenyl-, fluoro-substituted terphenyl-, tolane- and phenyl-tolane isothiocyanates liquid crystalline compounds feature high-birefringence, high polarity and low viscosity [1–5]. By combining several components one can control the properties of resulting liquid crystalline mixtures, such as birefringence, viscosity, refractivity indices, dielectric permittivity and elastic constants in accordance with requirements for various display and non-display applications. Further, the following material parameters of six different

recently produced medium- or high-birefringence liquid crystalline mixtures (HBLCM) are presented and discussed:

- W1898 (composed of two and three ring alkylcyclohexylbenzene and alkylbicyclohexylbenzene isothiocyanates),
- W1820 (composed of fluoro-substituted alkylbiphenyl- and alkylterphenyl isothiocyanates),
- W1852 (composed of fluoro-substituted alkylbiphenyl- and alkylcyclohexylbiphenyl- and alkylbicyclohexylbiphenyl isothiocyanates),
- W1825 and W1791 (composed on fluoro-substituted alkyltolane- and alkylphenyltolane isothiocyanates),
- W1865 (composed of fluoro-substituted alkylphenyl- and alkylbiphenyltolane isothiocyanates).

2. Experimental methods

The results of measurements and computations are collected in Table 1. Basic phase transition temperatures [°C] from crystal (or smectic A) to nematic (Cr–N) and from nematic to isotropic phase (N–I) for all mixtures were determined using the BIOLAR PI microscope equipped with the LINKAM 600 hot stage, controlled by the TMS 91 unit. Liquid (or bulk) viscosity Γ was defined at temperature T by using Ostwald capillary viscometer. Refractive indices of HBLCMs were measured with Abbe refractometer and when the values were higher than 1.87 or in the near infrared (NIR) region up to $\lambda = 1.060 \mu\text{m}$, the interference methods with the wedge-shaped cells were

Table 1. Material parameters of HBLCM mixtures at 25 °C.

	LC mixture					
	W1898	W1820	W1852	W1825	W1791	W1865
T [°C] (N–I)	83.5	71.1	152.6	136.0	127.5	170.1
T [°C] (Cr–N)	-20	10	-10	-12	-20	10
n_o at $\lambda = 0.589 \mu\text{m}$	1.51	1.52	1.53	1.54	1.54	1.54
Δn at $\lambda = 0.589 \mu\text{m}$	0.17	0.32	0.33	0.42	0.44	0.47
n_o at $\lambda = 1.064 \mu\text{m}$	1.50	1.51	1.52	1.53	1.53	1.53
Δn at $\lambda = 1.064 \mu\text{m}$	0.14	0.25	0.29	0.37	0.40	0.41
ε_{\perp} at $f = 1.5 \text{ kHz}$	3.5	5.5	4.1	4.7	4.5	5.0
$\Delta\varepsilon$ at $f = 1.5 \text{ kHz}$	8.1	19.5	15.3	17.0	16.4	18.2
K_{11} [pN]	12.0	13.5	11.2	12.5	21.2	10.5
K_{22} [pN]	7.5	8.2	7.7	7.4	8.3	7.8
K_{33} [pN]	24.1	33.0	31.0	32.1	25.2	29.4
K_{TN} [pN]	16.4	19.7	26.9	16.8	28.9	23.4
Γ [mPa s]	10	18	—	31	31	—
γ [mPa s]	97	180	320	284	213	595

Note: for W1865 the temperature of SmA–N transition instead of Cr–N one is given.

applied. Dielectric measurements were performed using the Hewlett-Packard type 4192A low frequency impedance analyzer for frequencies from 10 Hz to 10 MHz.

2.1. Measuring cells

In order to determine dielectric, electro-optic and some spectral characteristics of HBLCM samples, measurement cells of three types, with planar-homogeneous (or, HG), homeotropic (HT) and twisted nematic (TN) structure, were manufactured in our laboratory under WAT1 standard. The layout of such a cell is shown in Fig. 1.

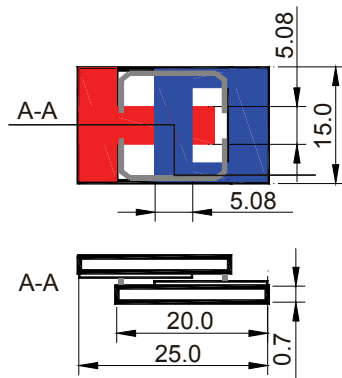


Fig. 1. Layout of a cell manufactured under WAT1 standard (one active area).

The bottom and top covers were prepared of high-quality float glass plates with thickness of 0.7 mm. The patterns of active areas ($5.08 \text{ mm} \times 5.08 \text{ mm}$) in all cells were etched in indium tin oxide (ITO) transparent layers deposited on glass substrates, with sheet resistances of 10, 70, and $500 \Omega/\text{sq}$, respectively. In the case of dispersive dielectric measurements the golden (Au) electrodes with sheet resistance smaller than $0.01 \Omega/\text{sq}$ were applied. Rubbed polyimides SE 130 and SE 1211 were applied as orienting coatings to obtain proper HG and TN (90° twist) or HT cells, respectively. The adhesive sealing material used in the manufacturing of these cells was rated to 180°C . In order to achieve a proper thickness d of the cells, spacers of 1.6, 2.5, 3.0, 5.0, 6.0, 7.0, 8.0 and $10.0 \mu\text{m}$ in thickness were added to the sealing material and sprayed at the active regions. Thickness and uniformity of the cells gap were measured by means of PREMA SPM 9001 spectrometer with the accuracy of $\pm 0.1 \mu\text{m}$. The label of the cell contains the thickness of the cell, orientation of LC texture and sheet resistance of the electrode layers. For example, 1.6HG10 indicates a cell gap of $1.6 \mu\text{m}$, planar-homogeneous orientation and ITO electrodes with sheet resistance of $10 \Omega/\text{sq}$ and 8.4HTAu indicates an $8.4 \mu\text{m}$ thick cell with homeotropic alignment and golden electrodes.

2.2. Dielectric permittivities

The temperature characteristics of real and imaginary parts of the isotropic $\varepsilon_l(T)$, perpendicular $\varepsilon_{\perp}(T)$ and parallel $\varepsilon_{||}(T)$ components of the permittivity tensors ε of

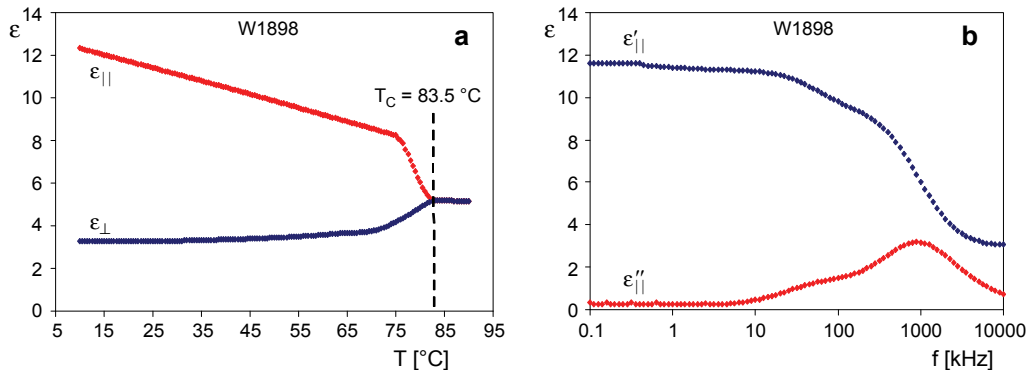


Fig. 2. Temperature dependences of real parts $\epsilon'_{||}(T)$ and $\epsilon'_\perp(T)$ for W1898 LC: at 25 °C and $f = 1$ kHz measured using: 5.4HGAu and 5.2HTAu cells, respectively (a) and 5.2HTAu cell (b).

HBLCMs were measured in nematic and isotropic phases. The temperature was stable to within 0.2 °C [6–8]. The results of dielectric and optical measurements for HBLCMs are further presented in figures and gathered in Tab. 1.

Typical temperature characteristics of real parts of $\epsilon'_\perp(T)$ and $\epsilon'_{||}(T)$ found for W1898 are shown in Fig. 2a. The results of dispersive measurements in the range from 100 Hz to 10 MHz for real $\epsilon'_{||}$ and imaginary $\epsilon''_{||}$ parts of $\epsilon_{||}$ for the same mixture at 25 °C are presented in Fig. 2b.

2.3. Refractive indices

Temperature characteristics of isotropic $n_i(T)$, ordinary $n_o(T)$ and extraordinary $n_e(T)$ refractive indices (up to $n = 1.87$) of HBLCMs were measured in nematic and isotropic phases (up to 130 °C) by an Abbe refractometer using light waves λ of 0.5007, 0.5400,

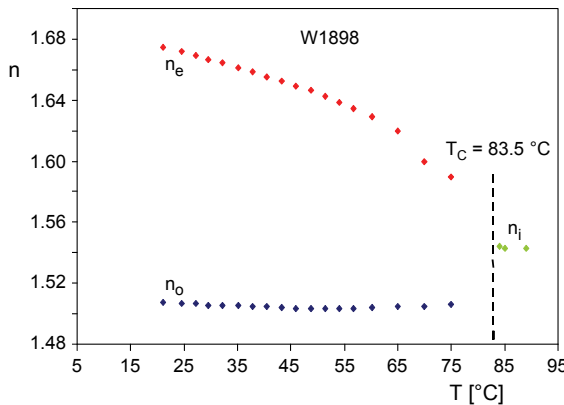


Fig. 3. Temperature dependence of $n_o(T)$, $n_e(T)$ and $n_i(T)$, for W1898 at yellow sodium line $\lambda = 0.5893 \mu\text{m}$ measured at 25 °C using Abbe refractometer.

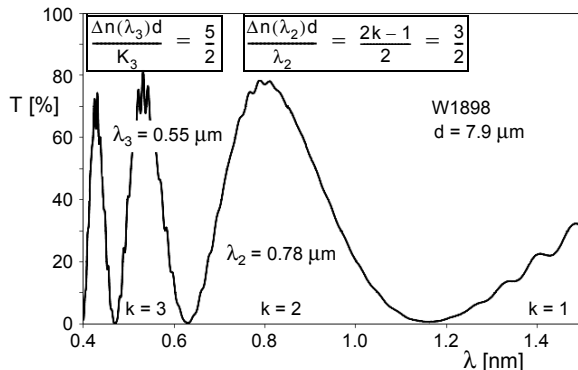


Fig. 4. Transmittance of W1898 at 25 °C in 7.9HG500 cell placed between crossed polarizers. The order k of a birefringent peak (maximum) at λ_k relates $\Delta n(\lambda_k)$ and cell thickness d [6, 11]; $\Delta n(\lambda_k) = (2k - 1)\lambda_k / 2d$.

0.5893, 0.6328, 0.6563 and 0.6731 μm. The measurement temperature in each step was stable to within 0.2 °C [9, 10]. The characteristics recorded for W1898 are shown in Fig. 3.

The measurements involving the interference method (Fig. 4) were performed by means of the JASCO V670 spectrometer. The magnitudes of refractive indices determined for HBLCMs under study are gathered in Table 1. When the measured refractive indices of HBLCMs were higher than 1.87 or in the near infrared (NIR) region up to $\lambda = 1.060$ μm, the interference methods with the wedge-shaped cells were

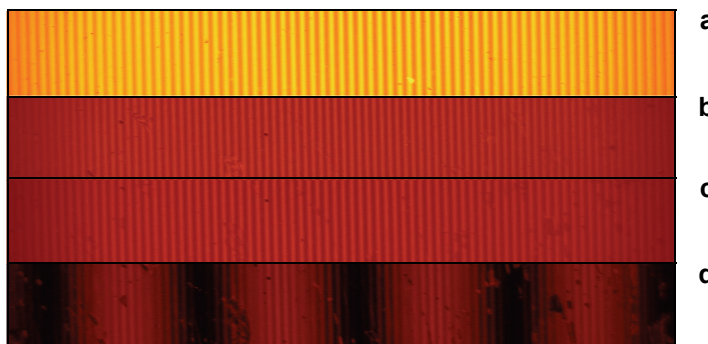


Fig. 5. Formation of interference fringes in a wedge cell for $\lambda = 0.6328$ μm at 25 °C: **a** – in the empty cell ($n = 1$, the distance of adjacent interference fringes $A = 0.0597$ mm is measured); **b** – in the cell filled with W1898 when direction of light polarization coincides with molecular director (then $n = n_e$, the distance between adjacent fringes $E = 0.0357$ mm is measured and $n_e = A/E = 1.672$ is calculated [10]); **c** – in the cell filled with W1898 when direction of light polarization is perpendicular to molecular director (then $n = n_o$ and the distance between adjacent interference fringes $O = 0.0396$ mm is measured and $n_o = A/O = 1.508$ is calculated); **d** – the cell placed between crossed polarizers (the molecular director of the layer forms angles of 45° with transmission axes), (the distance of adjacent interference fringes $B = 0.7067$ mm is measured and $\Delta n = 2A/B = 0.169$ is calculated).

applied [11, 12] (with wedge apex angle of order of a few milliradians). Interference fringes in wedge cells in visible (VIS) and NIR regions were recorded by CCD camera without NIR filter. The results of measurements and calculations of n_o , n_e and Δn of W1898 for $\lambda = 0.6328 \mu\text{m}$ at 25°C are illustrated in Fig. 5.

2.4. Elastic constants

The measurements of elastic constants K_{11} , K_{22} and K_{33} (corresponding to pure splay, twist and bend deformations) are usually based on determining critical magnitudes of electric (E_{1C} , E_{3C} , E_{5C} , E_{7C}) and magnetic (H_{2C} , H_{3C}) fields for different types of Fréedericksz transitions in proper HG, HT (see Figs. 6 and 7) or TN cells. Additionally, the reduced TN elastic constant K_{TN} (describing elasticity of LC layer in the transition from the twisted to homeotropic configuration) can be measured in the same way as K_{11} by using TN instead of HG cell. When dielectric ($\Delta\epsilon > 0$) and diamagnetic ($\Delta\chi > 0$) anisotropies of LCs are known, elastic constants can be calculated from the equation $K_{ii} = \pi^{-2}F_{ii}$, with factors F_{ii} corresponding to suitable configurations defined in Fig. 8. Magnetic field is necessary in some cases. Since diamagnetic ($\Delta\chi > 0$) anisotropies of mixtures under investigation are still unknown now, all elastic constants of HBLCMs were measured by exploiting only electric fields [12]. Figure 7 presents measurement geometries used for determining elastic constants when only electric fields are applied. To establish E_{5C} and E_{7C} (parallel to the boundary surfaces) in HG cell for twist and in HT cell for bend deformations, the interdigital electrodes are applied. Electric fields inside cells are formed using ITO in-plane switching type (IPS) electrodes in the form of rectangular stripes of width $b = 10 \mu\text{m}$ separated

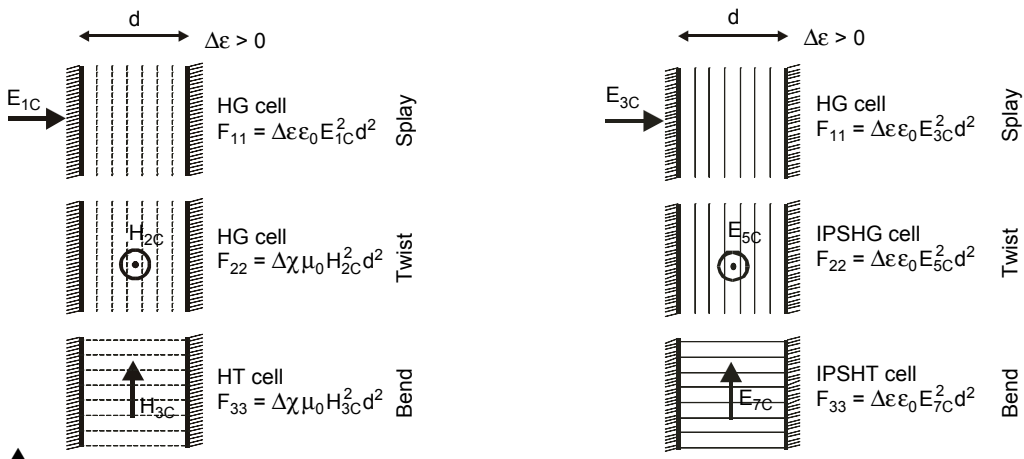


Fig. 6. Measurement geometries used for determining elastic constants K_{ii} when electric (E) and magnetic (H) fields are used (ϵ_0 and μ_0 are the electric and magnetic permittivity of free space).

Fig. 7. Measurement geometries used for determining elastic constants K_{ii} when only electric fields E are used.

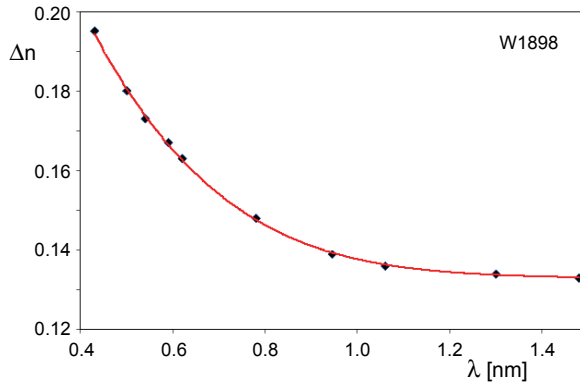


Fig. 8. Dispersion of optical anisotropy $\Delta n(\lambda)$ for W1898 at 25 °C. The selected points on the curve $\Delta n(\lambda)$ in VIS and NIR regions follow from values of $n_e(\lambda)$ and $n_o(\lambda)$ determined by combined methods, applying both appropriately prepared Abbe refractometer and interference wedges and being supported by interference methods [12].

by etched stripes of width $l = 20 \mu\text{m}$ in IPSHG or IPSHT cell of thickness around $d = 5 \mu\text{m}$. In the middle between the electrode stripes nearly homogeneous electric field $E_{5C} \approx U_{\text{th}}/l$ or $E_{7C} \approx U_{\text{th}}/l$ is induced by applying voltage U_{th} to interdigital electrodes [12]. Examples of determining elastic constants are given below. The constant magnitudes are gathered in Table 1.

2.4.1. Splay elastic constant

Figures 9 and 10 illustrate the Fréedericksz transition in HG cells filled with W1898 under voltage U at $f = 1 \text{ kHz}$ and 25 °C, monitored by dielectric and optical transmission measurements of the cell, respectively. In the case of optical measurement the cell was placed between crossed polarizers. The plane of polarization of incident

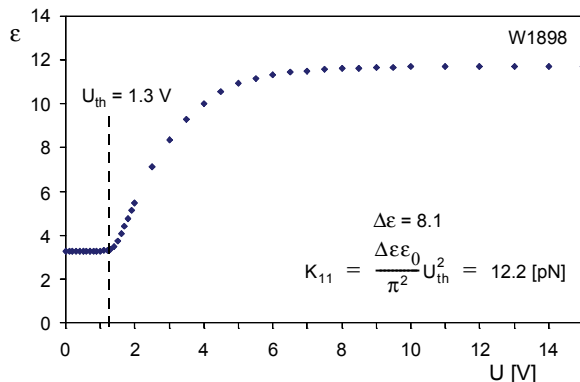


Fig. 9. Splay deformation of W1898 in 5.4HGAu cell. Effective dielectric permittivity was monitored by dielectric measurements.

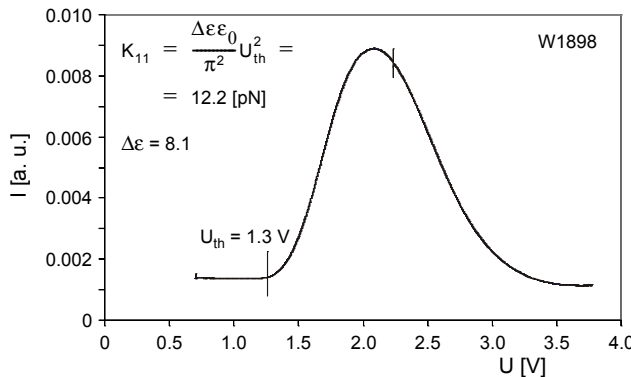


Fig. 10. Splay deformation in 5.4HG70 cell. Fréedericksz transition was monitored by light transmission measurements.

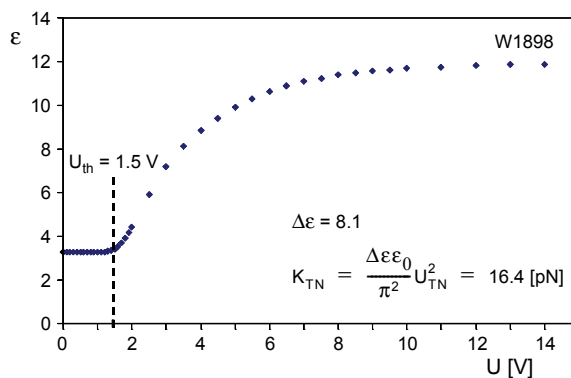


Fig. 11. Determination of K_{TN} reduced elastic constant from electric permittivity measurement in 3.1TN70 cell.

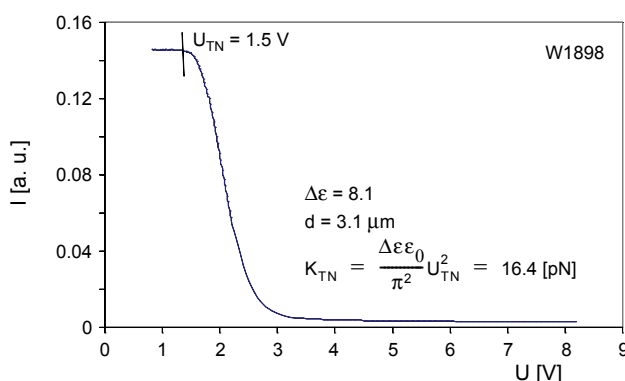


Fig. 12. Intensity I of light transmitted normally through 3.1TN70 cell.

light formed the angle of $\alpha = \pi/4$ with director **n** of HG LC layer. For both experiments the threshold voltages ($U_{\text{th}} = 1.3$ V) are the same; hence $F_{11} = \Delta\epsilon\epsilon_0 U_{\text{th}}^2$ and $K_{11} = \pi^{-2} F_{11}$.

2.4.2. Reduced elastic constant

Figures 11 and 12 illustrate the transition from twisted to homeotropic configuration in 3.1TN70 cell filled with W1898, controlled by voltage U and monitored by dielectric and optical transmission ($\lambda = 0.675$ μm) measurements in crossed polarizers, respectively. In both experiments the threshold voltages ($U_{\text{th}} = 1.5$ V) are the same resulting in the same value of $F_{\text{TN}} = \Delta\epsilon\epsilon_0 U_{\text{th}}^2$ and $K_{\text{TN}} = \pi^{-2} F_{\text{TN}}$.

2.4.3. Twist elastic constant

Twist deformation of W1898 layer in IPSHG cell (with thickness $d = 5.1$ μm) was monitored by optical measurements. Figure 13 shows the intensity I of the light

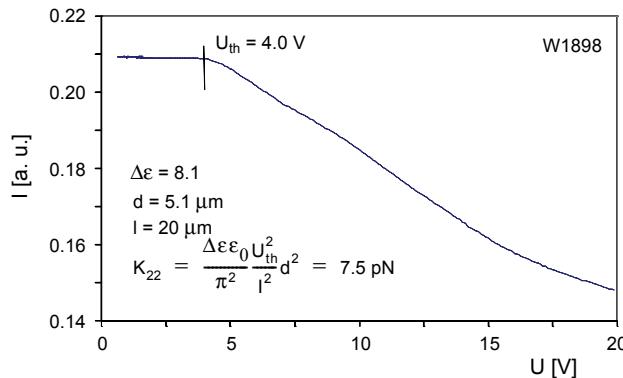


Fig. 13. Twist deformation of W1898 in a IPSHG cell of thickness $d = 5.1$ μm (intensity I of light with $\lambda = 656.3$ nm transmitted normally through the cell versus voltage U applied to the interdigital electrodes).

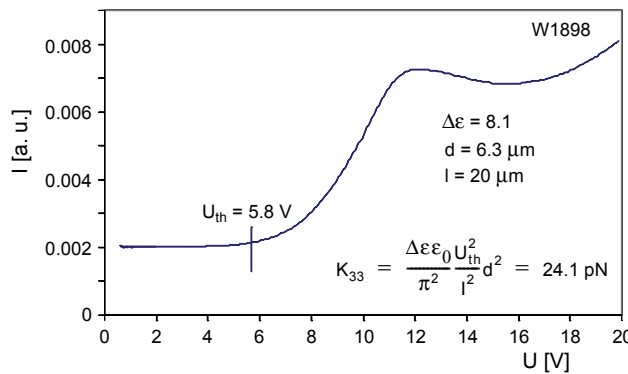


Fig. 14. Bend deformation of W1898 in an IPSHG cell of thickness $d = 6.3$ μm , determined from light ($\lambda = 0.589$ μm) transmitted through the cell placed between crossed polarizers.

transmitted through the cell versus voltage U applied to the interdigital electrodes. The cell was placed between crossed polarizers and the plane of polarization of incident light formed the angle of $\alpha = \pi/4$ with director \mathbf{n} of HG layer. Knowing the thickness d of IPSHG cell and the distance between the stripes of electrodes $l = 20 \mu\text{m}$, the twist elastic constant can be determined using the formula $K_{22} = \Delta\epsilon\epsilon_0\pi^2 U_{\text{th}}^2 l^{-2} d^2$.

2.4.4. Bend K_{33} elastic constant

Bend deformation of W1898 layer was monitored by optical measurements. Figure 14 shows the intensity I of light transmitted through an IPSHT cell of thickness $d = 6.3 \mu\text{m}$ versus voltage U applied to interdigital electrodes. The cell was placed between crossed polarizers. Given thickness d of the cell and the distance between the stripes of electrodes l , the bend elastic constant can be estimated as $K_{33} = \Delta\epsilon\epsilon_0\pi^2 U_{\text{th}}^2 l^{-2} d^2$.

2.5. Switching-on time and rotational viscosity

Rotational viscosity γ was estimated from measurements of the switching-on time $\tau_{\text{ON}} \approx \tau_{0.90}$ (see Fig. 15) of TN cells with a twist angle of 90° after applying an alternative voltage driving pulse of square shape. The rotational viscosity is calculated from Eq. (1) and Eq. (2) derived by TARUMI *et al.* [13]:

$$\gamma = \frac{\tau_{\text{ON}}(\epsilon_0\Delta\epsilon U^2 - \pi^2 K_{\text{TN}})}{d^2} \quad (1)$$

where d is the cell gap, U is the amplitude of driving voltage applied to the cell and K_{TN} is the reduced elastic constant for the transition from twisted to homeotropic

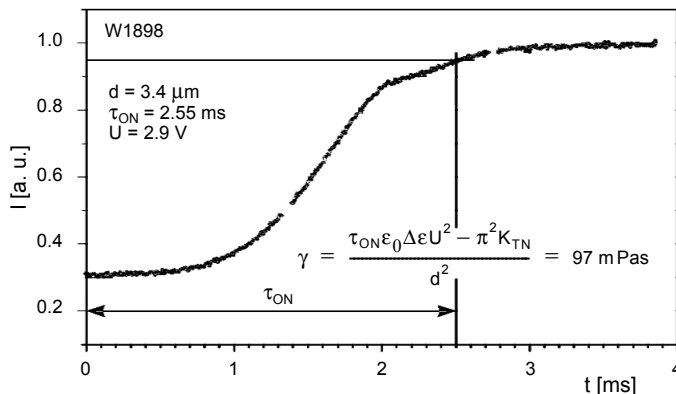


Fig. 15. Fréedericksz transition versus time in 3.4TN70 cell filled with W1898 mixture.

configuration in TN cell. These results were verified by study of the switching-off times $\tau_{\text{OFF}} \approx \tau_{100-10}$.

$$\gamma = \frac{\tau_{\text{OFF}} \pi^2 K_{11}}{d^2} \quad (2)$$

where K_{11} is the elastic constant for splay deformation.

The values of the rotational viscosity γ obtained from the last formula applied for HG cell filled with W1898 mixture were consistent with the former ones. The maximal discrepancy between the results obtained using the two methods was below 10%.

3. Results for other mixtures

Using the procedures described in the previous sections the following results for temperature dependences of permittivity and dispersion of optical anisotropy were obtained for other mixtures. As was mentioned above, temperature dependences of real parts (parallel and perpendicular to director) of permittivity were measured at a frequency of 1 kHz using HG and HT cells with low resistivity electrodes. The characteristics of dielectric permittivity versus frequency for all the mixtures

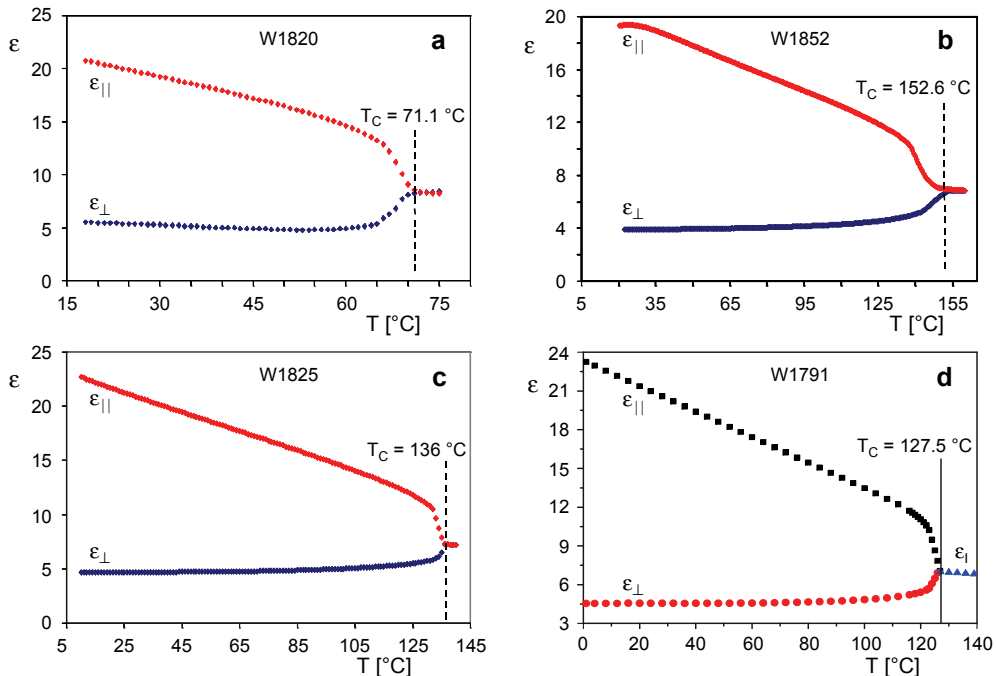


Fig. 16. To be continued on the next page.

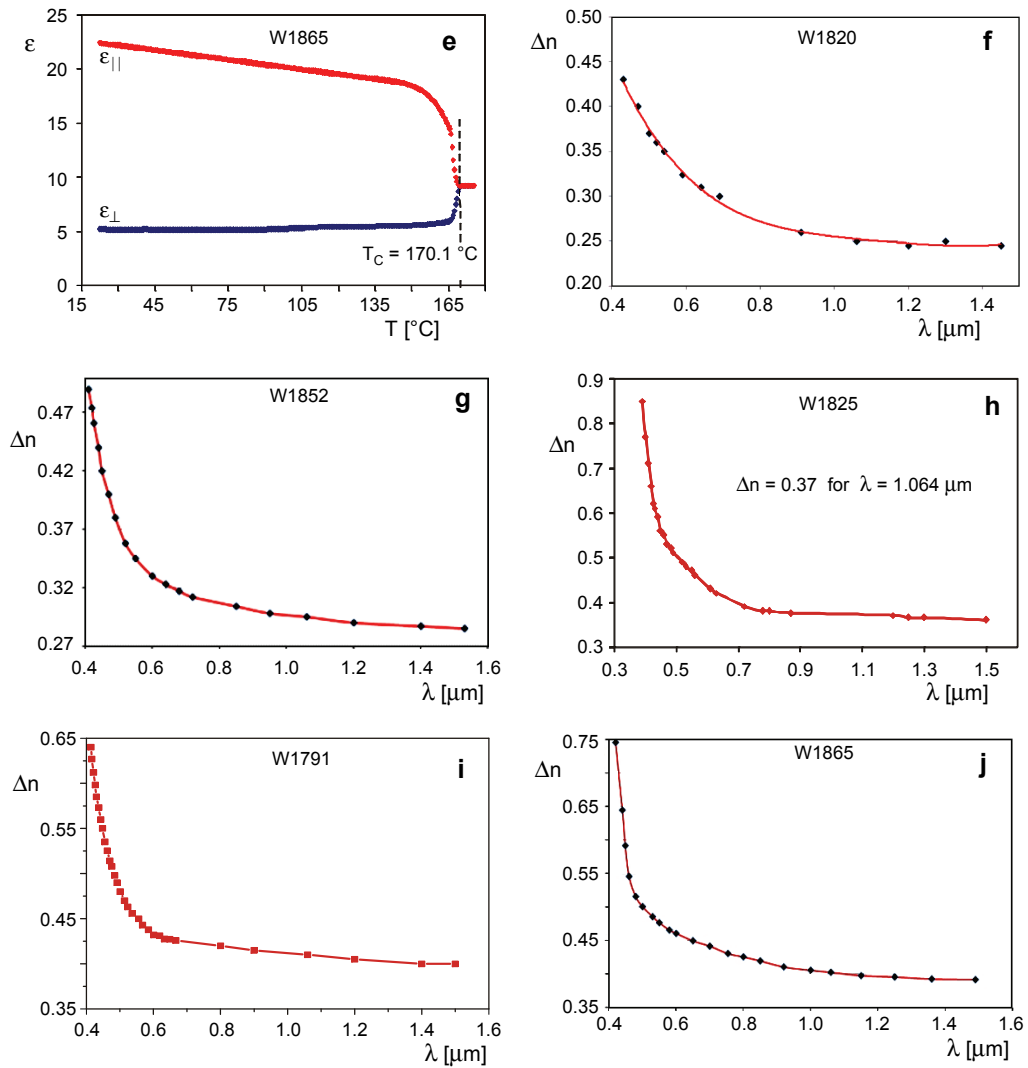


Fig. 16. Temperature dependences of permittivity (a–e) and dispersion of optical anisotropy (f–j) for W1820, W1852, W1825, W1791 and W1865 mixtures, respectively.

investigated were very similar to those shown in Figs. 2a and 2b for the W1898 mixture. Curves for dispersion of optical anisotropy were obtained by combining the results from Abbe refractometer, wedge-cell and spectroscopic measurement at 25 °C. The results are shown in Fig. 16.

4. Summary

The results of measurements characterising dielectric, refractive, elastic and viscous properties of the HBLCMs studied are gathered in Table 1. Due to the high optical and

dielectric anisotropies and relatively low rotational viscosities of these mixtures, they can be applied in different kinds of liquid crystal electro-optical devices with low response times, operating in visible and near infrared regions. For example:

– The W1825 LC with $\Delta n = 0.37$ at $\lambda = 1.064 \mu\text{m}$ can be exploited in producing liquid crystal cell (LCC) to be applied in space-borne laser rangefinder for space missions. Such LCC may operate in the positive TN mode tuned to first TN maximum ($d = 3^{1/2}\lambda/(2\Delta n) = 2.5 \mu\text{m}$), switching the polarization plane of laser beam with work wavelength of $1.064 \mu\text{m}$ and the energy density not smaller than 0.15 J/cm^2 at the pulse duration about 8 ns. Transmission of LCC should be not smaller than 85% (see Fig. 12) at the working aperture not less than 15 mm. The switching on and switching off times in a $2.5 \mu\text{m}$ thick LCC driven by voltage of 10 V are not longer than 0.7 ms and 7 ms, respectively, in operating temperature range from 20°C to 60°C [14].

– The W1791 LC with $\Delta n > 0.40$ up to $\lambda = 1.5 \mu\text{m}$ can be exploited in electrically tunable liquid crystal filters (ETLCF). Due to relatively high and electrically controlled optical anisotropies $\Delta n(U)$ and thin cell gaps d ($1 \mu\text{m}$, $3 \mu\text{m}$ and $5 \mu\text{m}$) applied in ETLCF with W1791, one can select the required wavelength $\lambda(U)$ from visible up to near infrared spectrum range [15]. The ETLCF can achieve the response time shorter than 1 ms in temperature range from 20°C to 60°C .

– The W1898 LC with $\Delta n = 0.17$ at $\lambda = 0.589 \mu\text{m}$ can be used for producing liquid crystal light valve (LCLV). Such LCLV may operate in electrically controlled birefringence mode, tuned to first maximum ($d = \lambda/(2\Delta n) = 1.7 \mu\text{m}$), in the whole visible range. The switching on and switching off times in a $1.5 \mu\text{m}$ thick LCLV with W1898 driven by voltage of 10 V are not longer than 0.4 ms and 4 ms, respectively, in operating temperature range from 20°C to 60°C .

Acknowledgements – This work was supported by the Grant No. NN507 471837 from the Polish Ministry of Science and Higher Education.

References

- [1] DĄBROWSKI R., DZIADUSZEK J., SZCZUCIŃSKI T., *Mesomorphic characteristics of the some new homologous series with the isothiocyanato terminal group*, Molecular Crystals and Liquid Crystals **124**(1), 1985, pp. 241–257.
- [2] SPADŁO A., DĄBROWSKI R., FILIPOWICZ M., BOGUN M., GAUZA S., WU S.T., *Synthesis, mesomorphic and optical properties of 4'-alkyl-3,5-difluoro-4-isothiocyanatotoluenes and 4'-alkylphenyl-3,5-difluoro-4-isothiocyanatotolanes*, Conference Proceedings, XVI Conference on Liquid Crystals, Stare Jabłonki, 2005, Poland, pp. 53–58.
- [3] DĄBROWSKI R., DZIADUSZEK J., ZIÓŁEK A., SZCZUCIŃSKI Ł., STOLARZ Z., SASNOUSKI G., BEZBORODOV V., LAPANIĆ W., GAUZA S., WU S.T., *Low viscosity, high birefringence liquid crystalline compounds and mixtures*, Opto-Electronics Review **15**(1), 2007, pp. 47–51.
- [4] GAUZA S., WEN C.H., WU B., WU S.T., SPADŁO A., DĄBROWSKI R., *High figure-of-merit nematic mixtures based on totally unsaturated isothiocyanate liquid crystals*, Liquid Crystals **33**(6), 2006, pp. 705–710.
- [5] DĄBROWSKI R., DZIADUSZEK J., GARBAT K., FILIPOWICZ M., URBAN S., GAUZA S., SASNOUSKI G., *Synthesis and mesogenic properties of three- and four-ring compounds with a fluoroisothiocyanatobiphenyl moiety*, Liquid Crystals **37**(12), 2010, pp. 1529–1537.

- [6] RASZEWSKI Z., *Measurement permittivity of liquidcrystalline substances*, Electron Technology **20**, 1987, pp. 99–113.
- [7] PERKOWSKI P., *Dielectric spectroscopy of liquid crystals. Theoretical model of ITO electrodes influence on dielectric measurements*, Opto-Electronics Review **17**(2), 2009, pp. 180–186.
- [8] BARAN J.W., RASZEWSKI Z., DĄBROWSKI R., KĘDZIERSKI J., RUTKOWSKA J., *Some physical properties of mesogenic 4-(trans-4'-n-alkylcyclohexyl)-isothiocyanobenzenes*, Molecular Crystals and Liquid Crystals **123**(1), 1985, pp. 237–245.
- [9] KĘDZIERSKI J., KOJDECKI M.A., RASZEWSKI Z., ZIELIŃSKI J., LIPIŃSKA L., *Determination of anchoring energy, diamagnetic susceptibility anisotropy and elasticity of some nematics by means of semiempirical metod of self-consistent director field*, Proceedings of SPIE **6023**, 2005, article 602305.
- [10] KĘDZIERSKI J., RASZEWSKI Z., KOJDECKI M.A., KRUSZELNICKI-NOWINOWSKI E., PERKOWSKI P., PIECEK W., MISZCZYK E., ZIELIŃSKI J., MORAWIAK P., OGRODNIK K., *Determination of ordinary and extraordinary refractive indices of nematic liquid crystals by using wedge cells*, Opto-Electronics Review **18**(2), 2010, pp. 214–218.
- [11] MISZCZYK E., RASZEWSKI Z., KĘDZIERSKI J., NOWINOWSKI-KRUSZELNICKI E., KOJDECKI M.A., PERKOWSKI P., PIECEK W., OLIFIERCZUK M., *Interference method for determining dispersion of refractive indices of liquid crystals*, Molecular Crystals and Liquid Crystals **544**(1), 2011, pp. 22–36.
- [12] KĘDZIERSKI J., RASZEWSKI Z., NOWINOWSKI-KRUSZELNICKI E., KOJDECKI M.A., PIECEK W., PERKOWSKI P., MISZCZYK E., *Composite method for measurement of splay, twist and bend nematic elastic constants by use of single special in-plane-switched cell*, Molecular Crystals and Liquid Crystals **544**(1), 2011, pp. 56–68.
- [13] TARUMI K., FINKENZELLER U., SCHULER B., *Dynamic behaviour of twisted nematic liquid crystals*, Japanese Journal of Applied Physics Part 1 **31**(9A), 1992, pp. 2829–2836.
- [14] NOWINOWSKI-KRUSZELNICKI E., JAROSZEWCZ L., RASZEWSKI Z., SOMS L., PIECEK W., PERKOWSKI P., KĘDZIERSKI J., DĄBROWSKI R., OLIFIERCZUK M., MISZCZYK E., *Liquid crystal cell for space-borne laser rangefinder to space mission applications*, Opto-Electronics Review, 2011, (in press).
- [15] RASZEWSKI Z., KRUSZELNICKI-NOWINOWSKI E., KĘDZIERSKI J., PERKOWSKI P., PIECEK W., DĄBROWSKI R., MORAWIAK P., OGRODNIK K., *Electrically tunable liquid crystal filters*, Molecular Crystals and Liquid Crystals **525**(1), 2010 pp. 112–127.

Received September 4, 2011
in revised form October 24, 2011